Molecular Therapy
Methods & Clinical Development
Original Article

Long-Term Therapeutic Efficacy of Intravenous AAV-Mediated Hamartin Replacement in Mouse Model of Tuberous Sclerosis Type 1

Shilpa Prabhakar,[1] Pike See Cheah,[1,6] Xuan Zhang,[1] Max Zinter,[1] Maria Gianatasio,[2] Eloise Hudry,[1] Roderick T. Bronson,[3] David J. Kwiatkowski,[4] Anat Stemmer-Rachamimov,[2] Casey A. Maguire,[1] Miguel Sena-Esteves,[5] Bakhos A. Tannous,[1] and Xandra O. Breakefield[1]

[1]Molecular Neurogenetics Unit, Department of Neurology and Center for Molecular Imaging Research, Department of Radiology, Massachusetts General Hospital, and Neurodiscovery Center, Harvard Medical School, Charlestown, MA, USA; [2]Department of Pathology, Massachusetts General Hospital, Boston, MA, USA; [3]Rodent Histopathology Core Facility, Harvard Medical School, Boston, MA, USA; [4]Brigham and Women's Hospital, Harvard Medical School, Boston, MA, USA; [5]Department of Neurology, Horae Gene Therapy Center, University of Massachusetts Medical School, Worcester, MA, USA; [6]Department of Human Anatomy, Faculty of Medicine and Health Sciences, Universiti Putra Malaysia, Selangor, Malaysia

Tuberous sclerosis complex (TSC) is a tumor suppressor syndrome caused by mutations in *TSC1* or *TSC2*, encoding hamartin and tuberin, respectively. These proteins act as a complex that inhibits mammalian target of rapamycin (mTOR)-mediated cell growth and proliferation. Loss of either protein leads to overgrowth in many organs, including subependymal nodules, subependymal giant cell astrocytomas, and cortical tubers in the human brain. Neurological manifestations in TSC include intellectual disability, autism, hydrocephalus, and epilepsy. In a stochastic mouse model of TSC1 brain lesions, complete loss of *Tsc1* is achieved in homozygous *Tsc1*-floxed mice in a subpopulation of neural cells in the brain by intracerebroventricular (i.c.v.) injection at birth of an adeno-associated virus (AAV) vector encoding Cre recombinase. This results in median survival of 38 days and brain pathology, including subependymal lesions and enlargement of neuronal cells. Remarkably, when these mice were injected intravenously on day 21 with an AAV9 vector encoding hamartin, most survived at least up to 429 days in apparently healthy condition with marked reduction in brain pathology. Thus, a single intravenous administration of an AAV vector encoding hamartin restored protein function in enough cells in the brain to extend lifespan in this TSC1 mouse model.

INTRODUCTION

Tuberous sclerosis complex (TSC) is an autosomal-dominant, tumor suppressor disorder caused by an inherited or *de novo* mutation in one allele of *TSC1* (encoding hamartin) or *TSC2* (encoding tuberin), which affects 2 million people worldwide with an incidence of 1/6,000 live births.[1] Hamartin and tuberin act as a complex with Tre2-Bub2-Cdc16 (TBC) 1 domain family, member 7 (TBC1D7) with Rheb-GAP activity to inhibit mammalian target of rapamycin complex 1 (mTORC1), which in turn regulates cell growth and proliferation.[2] Mutation of the corresponding normal allele of *TSC1* or *TSC2* in somatic cells leads to hamartoma (tumor) development in many organs, including brain, heart, kidneys, skin, and lungs.[3,4] Most TSC patients have neurological involvement (95%), including cortical tubers, subependymal nodules (SENs), and subependymal giant cell astrocytomas (SEGAs), with symptoms including epilepsy (85%), autism (40%), cognitive impairment (50%), and developmental delay (70%).[5] Rapamycin and rapalog therapy, which partially inhibits mTORC1, has been shown to be effective for several aspects of TSC pathophysiology, but may interfere with normal brain development, including neuronal growth, axon guidance, synapse formation, and myelination.[6,7] Furthermore, rapalog therapy must be continuous or growth of lesions will resume.

In previous studies, we demonstrated that a single intracerebroventricular (i.c.v.) injection of an adeno-associated virus (AAV) serotype rh8 vector encoding human hamartin under the cytomegalovirus (CMV) promoter[8] into pups at post-natal day (P) 0 could effectively rescue neurodevelopment and extend survival from a mean of 22–52 days in offspring of homozygous *Tsc1*$^{c/c}$*ROSA* (hereafter referred to as *Tsc1*-floxed) expressing Cre under the synapsin promoter.[9] In this model, hamartin is lost in all brain neurons commencing during development at embryonic day 12.[10]

In order to more realistically model brain lesions in TSC1 patients that arise from loss of hamartin in a subset of cells of different types in the brain, including neural precursor cells, neurons, astrocytes, and subependymal cells, we developed a stochastic mouse model in which loss of hamartin is random in a subpopulation of cells throughout the

Received 7 February 2019; accepted 14 August 2019;
https://doi.org/10.1016/j.omtm.2019.08.003.

Correspondence: Xandra O. Breakefield, PhD, Molecular Neurogenetics Unit, Department of Neurology and Center for Molecular Imaging Research, Department of Radiology, Massachusetts General Hospital-East, 13th Street, Building 149, Charlestown, MA 02129, USA.
E-mail: breakefield@hms.harvard.edu

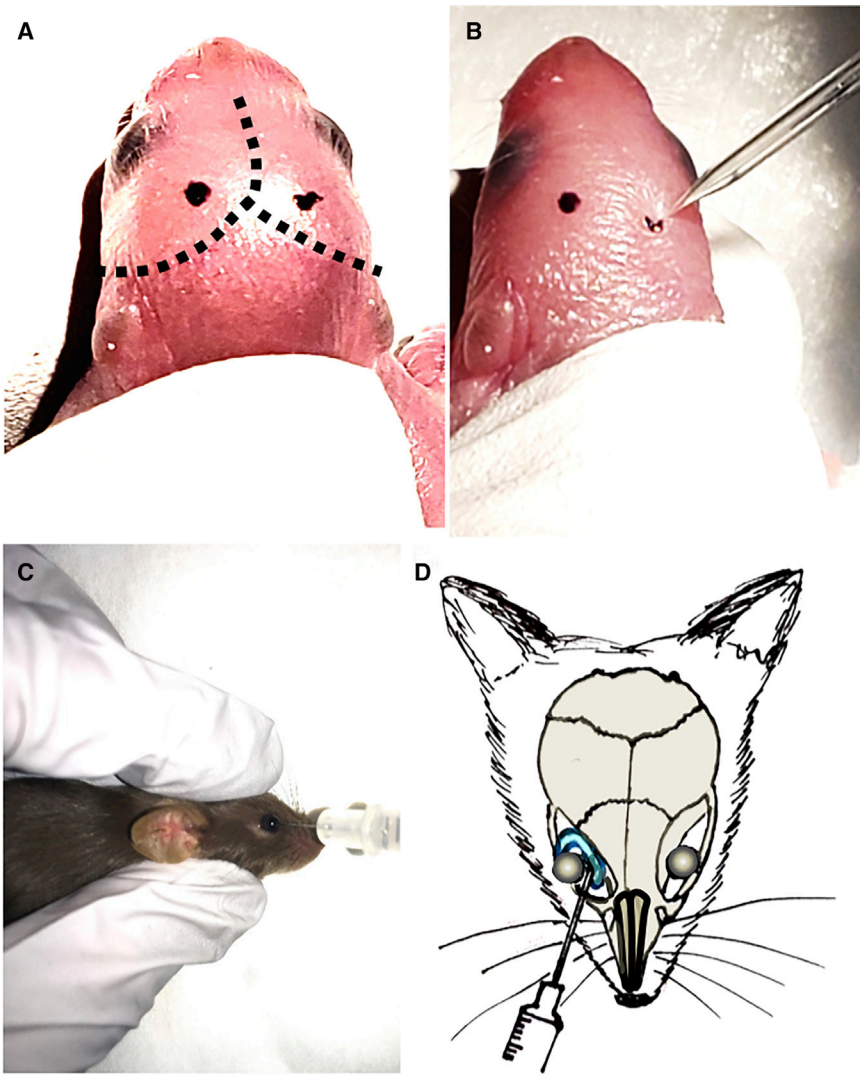

Figure 1. Schematic Representation of the Injection Paradigms

(A) Landmarks such as sagittal and lambdoid sutures are visible through the skin of a newborn pup (dotted lines). The i.c.v. injection sites (black dots) were marked with a non-toxic laboratory pen. (B) i.c.v. injection was made using a finely pulled glass pipette. (C) For i.v. injections, the needle was inserted, bevel down, at the medial canthus, into the retro-orbital sinus. (D) Diagram shows correct placement of the needle relative to the retro-orbital sinus, the eyeball, and the back of the orbit.

brain, and possibly in other parts of the body, starting at P0.[11] This model was achieved by i.c.v. injection of an AAV serotype 1 vector encoding Cre recombinase under the constitutive chicken β-actin (CBA) promoter[8] into *Tsc1*-floxed pups at P0. We documented heterotopic brain lesions, enlarged neurons, and the formation of subependymal lesions and enlarged ventricles leading to hydrocephalus and early death.[11]

Here we demonstrate the benefit of gene replacement in this stochastic *Tsc1*-floxed mouse model. Tsc1 loss was induced in a subset of neural cells by i.c.v. injection of AAV1-Cre at P0, and then these mice were injected intravenously (i.v.) at P21 with AAV serotype rh8 or 9 vectors encoding human hamartin under the CMV promoter, or with a control vector or no vector. Behavior, survival, neuropathology, and whole-body pathology were accessed. Advantages of a gene replacement approach using AAVrh8 or AAV9 include the possible effectiveness of a single systemic injection of vector, low toxicity, extensive biodistribution, and ability to cross the blood-brain barrier (BBB).[12,13]

RESULTS

The vector used for hamartin delivery has AAV2 inverted terminal repeats (ITRs) and human hamartin cDNA tagged with a c-Myc epitope under a CMV promoter.[9] A parallel construct encoding GFP was used as a control.[14] The plasmid constructs were transfected into HEK293 cells, and cell lysates were used for western blots showing a band corresponding to hamartin-c-Myc (135 kDa) using antibodies to either hamartin or c-Myc.[9] These constructs were then packaged in either AAVrh8 or AAV9 capsids. i.c.v. injection of the AAV1-CBA-Cre vector (Figures 1A and 1B) was performed in newborn pups, followed by i.v. injection of the AAV-CMV-hamartin vector into the retro-orbital vasculature at P21 (Figures 1C and 1D).

In the first set of experiments, homozygous *Tsc1*-floxed P0 pups were injected i.c.v. with AAV1-Cre, using 2 μL containing 9.6×10^9 genome copies (g.c.), into each ventricle (total of 1.9×10^{10} g.c.). These mice were injected i.v. on P21 with 60 μL total volume of AAVrh8-hamartin (10 μL containing 2×10^{10} g.c. + 50 μL saline; n = 12) or AAVrh8-GFP (1 μL containing 1.2×10^{10} g.c. + 50 μL saline; n = 12) into the retro-orbital vasculature behind one eye or received no injection (n = 5). The g.c. ratio of i.c.v. to i.v. AAV was about 1:6. Average survival time for the AAVrh8-GFP-injected or non-i.v.-injected mice was 47 days, whereas mice injected with AAVrh8-hamartin had extended average survival to 156 days ($p < 0.0001$) (Figure 2A). Over 40 days after P0 AAV1-Cre i.c.v. injection, *Tsc1*-floxed mice had enlarged heads indicative of brain hydrocephalus and hunched backs associated with distress, as compared with those subsequently treated with i.v. AAV-hamartin, which appeared similar to normal mice (n = 5/group; Figure S1). No signs of overt epilepsy were observed in handling the mice. In both sets of experiments (one set injected with AAVrh8-hamartin and the other set injected with AAV9-hamartin at P21), mice from

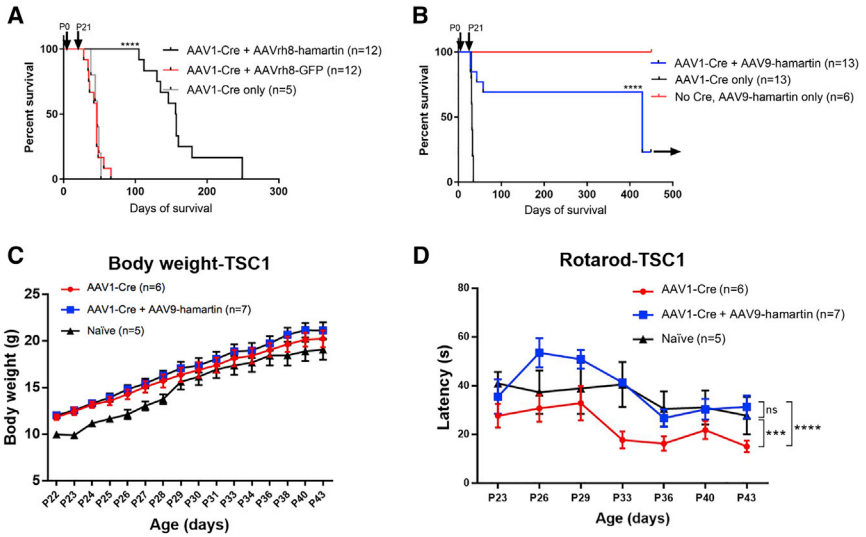

Figure 2. Gene Replacement and Survival of *Tsc1*-Floxed Mice Injected with AAV-Cre Vectors with and without AAV-Hamartin Vectors, Including Body Weight and Rotarod Assessments

(A) Homozygous *Tsc1*-floxed pups received i.c.v. injection into both cerebral ventricles at P0 using the AAV1-Cre vector. At P21 in four separate experiments, mice were randomly assigned into three groups for retro-orbital injections (group 1 = mice injected with AAVrh8-hamartin [n = 12]; group 2 = mice injected with AAVrh8-GFP [n = 12]; group 3 = no injection [n = 5]). Log-rank (Mantel-Cox) survival curves were 156, 46, and 47 days for groups 1, 2, and 3, respectively. A highly significant difference, $p < 0.0001$ (log-rank test; GraphPad Prism), was found when comparing group 1 with groups 2 and 3. (B) Homozygous *Tsc1*-floxed pups received i.c.v. injection into both cerebral ventricles at P0 using the AAV1-Cre vector. At P21 days, in three separate experiments mice were randomly assigned to three groups for retro-orbital injections (group 1 = AAV-Cre + AAV9-hamartin [n = 13]; group 2 = no injection [n = 13]). Another set of mice (group 3) was injected with only AAV9-hamartin at P21 days with no Cre injection (n = 6). Mean survival, based on log-rank (Mantel-Cox) survival curves, in the different groups was 429, 32, and >450 days for groups 1, 2, and 3, respectively. Black arrow indicates when mice were sacrificed. A highly significant difference, $p < 0.0001$ (log-rank test, GraphPad Prism), was found when comparing groups 1 and 2. Groups 1 and 3 were also significantly different, $p < 0.005$. (C) Tsc1-floxed mice injected with AAV1-Cre vector with (n = 7) and without (n = 6) AAV9-hamartin vector showed normal weight gain as compared with naive mice (n = 5). (D) At an accelerated speed of 4–64 rpm for the rotarod test, the motor function of the Tsc1-floxed mice rescued by AAV9-hamartin vector was similar to the control and significantly decreased as compared with the AAV1-Cre-only group. ***$p < 0.001$; ****$p < 0.001$ (two-way ANOVA test).

each group (n = 3/group) were examined at P37 by a rodent pathologist (R.T.B.), and no pathology was observed in any organs throughout the body.

In a second set of experiments, *Tsc1*-floxed pups were injected i.c.v. with AAV1-Cre, using 2 μL containing 1.6×10^{10} g.c., into each ventricle (total of 3.2×10^{10} g.c.) at P0. AAV-Cre-injected mice that did not receive an i.v. vector injection (n = 13) died on average by day 32. Most mice subsequently injected i.v. at day 21 with a total volume of 60 μL AAV9-hamartin (10 μL containing 2.4×10^{11} g.c. + 50 μL saline; n = 13) into the retro-orbital vasculature behind one eye lived over 400 days (at least a 10-fold increase in survival time), at which point they were sacrificed for pathology (Figure 2B, arrow). The g.c. ratio of i.c.v. to i.v. AAV was about 1:7.5. All mice that did not receive the AAV-Cre injection at P0 but did receive the AAV9-hamartin in a total volume of 60 μL (10 μL containing 2.4×10^{11} g.c. + 50 μL saline; n = 6) lived up to at least 450 days, supporting low-to-no toxicity of this hamartin vector (Figure 2B). Because the AAV9 vector appeared to be more effective than the AAVrh8 vector in extending lifespan in this Tsc1 model, we used AAV9 for subsequent experiments.

In the next set of experiments, *Tsc1*-floxed pups were injected i.c.v. with AAV1-Cre, using 2 μL containing 1.8×10^{11} g.c., into each ventricle (total of 3.6×10^{11} g.c.) at P1 (n = 13). At P21, half of the mice were injected with AAV9-hamartin (20 μL containing 1.5×10^{12} g.c. + 40 μL saline; n = 7) into the retro-orbital vasculature behind one eye, and the other half of mice were non-injected. These mice at P23 were subjected to body weight measurement and motor function assessment (n = 5 for naive group [male = 2; female = 3], n = 6 for AAV1-CBA-Cre injection at P1 [male = 2; female = 4], n = 7 for AAV1-Cre injection at P1 and AAV9-hamartin injection at P21 [male = 3; female = 4]). Body weights of the animals were recorded over the period of P23–P43 with similar rates of weight gain in all groups (Figure 2C). Movement was assessed using an automated rotarod apparatus using accelerated (4–64 rpm over 120 s) velocities. A significant decreased time to fall off the rotarod (latency) was observed for the AAV1-Cre-injected mice as compared with the AAV1-Cre+AAV9-hamartin and control mice (Figure 2D).

Neuropathological examination of mouse brains from the experiments revealed enlarged ventricles and clumping of subependymal cells, suggesting proliferation, in many areas around the ventricles on day 37 after i.c.v. AAV1-Cre injection of *Tsc1*-floxed pups (Figures 3B and 3E), as compared with normal non-injected mice (Figures 3A and 3D). Brain pathology in the former was resolved following P21 i.v. injection of the AAV9-hamartin vector (Figures 3C and 3F). Immunostaining with Ki67 of the mouse brains (Figures 4A–4C), mounted using DAPI counterstain media (Figures 3D–3F), revealed more proliferating cells in the ependymal and subependymal layers around the ventricles, with some moving away from the ventricles on day 43 after i.c.v. AAV-Cre injection of *Tsc1*-floxed pups (Figure 4B), as compared with normal non-injected mice (Figure 4A) or mice injected with the AAV1-Cre vector followed by the AAV9-hamartin vector (Figure 4D).

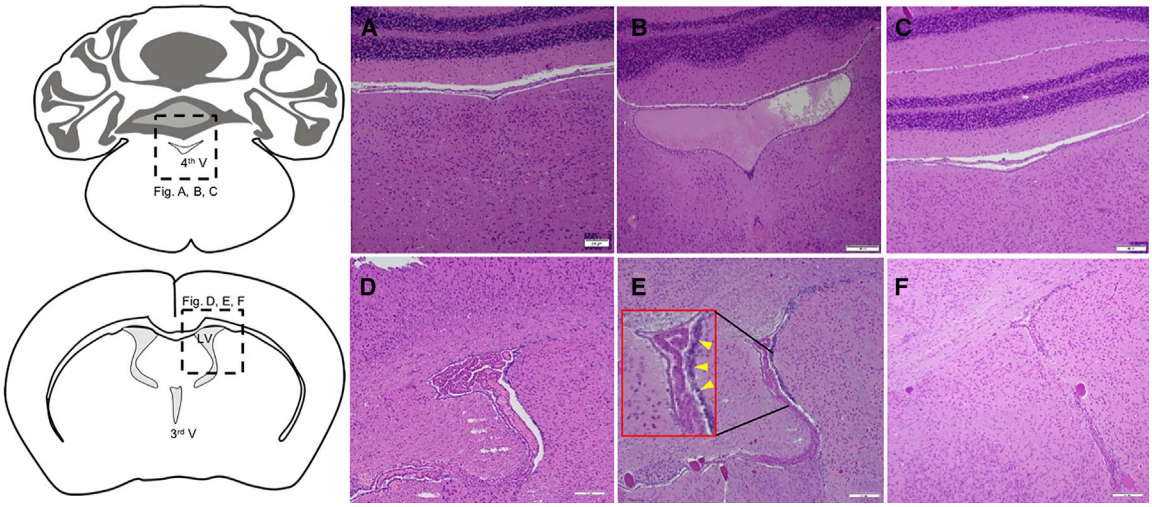

Figure 3. H&E Staining of *Tsc1*-Floxed Brains

(A–F) Coronal section of the fourth (4th V) (A–C) and third ventricles (3rd V) (D–F). (A and D) Coronal sections of normal non-injected *Tsc1*-floxed brains at P37 showed normal-sized ventricles (A) and the subependymal layer (D). (B and E) *Tsc1*-floxed mice injected i.c.v. with AAV1-Cre on P0 exhibited enlarged ventricle, indicating incipient hydrocephalus (B) and cell clumping, indicating overgrowth of subependymal cells lining the ventricle (E, inset: arrowheads showing the higher magnification of clumping of subependymal cells). (C and F) *Tsc1*-floxed mice injected i.c.v. with AAV1-Cre on P0, then retro-orbitally injected with AAV9-hamartin at P21 showed normal ventricular size (C) and a single subependymal layer of cells surrounding the ventricles (F). Original magnification, ×10. Scale bars, 200 μm.

The average increase in neuronal cell size in the brain resulting from i.c.v. AAV1-Cre injection (Figure 5B) was restored to normal size (Figure 5A) after i.v. injection of AAV9-hamartin at P21, as assessed on P37 (Figure 5C). This histological observation was further supported by data quantified blindly by measuring neuronal cell area and perimeter (Figure 5D), with H&E-stained neurons identified in cortical sections as having a prominent nucleolus within a pale staining nucleus and cytoplasm.[15] Phosphorylation of S6 is upregulated in TSC-deficient cells as a result of loss of hamartin and increase in mTORC1 activity.[9] In the present study, elevated pS6 immunostaining was evaluated in the cerebral cortex of AAV1-Cre injected *Tsc1*-floxed pups (Figure S2B), as compared with AAV9-hamartin-injected mice (Figure S2C) and normal controls (Figure S2A). Quantitative analysis of pS6 staining was carried out by blinded scoring of staining intensity. Although there was a trend for lower staining intensity in non-injected and AAV-Cre/AAV9-hamartin mice as compared with AAV-Cre-only-injected mice, the difference among groups was not significant (Figure S2D).

In order to assess the extent and types of cells in the brain in which the AAV1-mediated delivery of Cre-recombinase might lead to loss of hamartin, we used the floxed reporter mouse [Gt(ROSA)26Sor$^{tm9(CAG\text{-}tdTomato)Hze}$], which was injected with 2 μL containing 1.8×10^{11} g.c. (total of 3.6×10^{11} g.c.) AAV1-CBA-Cre i.c.v. into each ventricle of P1 pup. At P21, the animals were euthanized, and red fluorescent cells were evaluated by fluorescent microscopy (Figure S3A). Extensive delivery was noted throughout the brain, including cells with the morphology of neurons (yellow arrowhead, Figure S3A′) and astrocytes (white arrowhead, Figure S3A′) in the cerebral cortex (Figure S3A′), cells in the hippocampus (Figure S3A″), as well as cells adjacent to the ventricular region (Figure S3A″). In order to investigate the efficiency of i.v. delivery of AAV9, AAV9-CBA-GFP (1.8×10^{11} g.c. in 60 μL) was administered into the retro-orbital vein of P21 pups. Two weeks later, the animals were sacrificed, and GFP-positive cells were studied. We observed efficient delivery of virus vector in which GFP-positive cells were found throughout the brain including those appearing to be neurons (yellow arrowhead, Figure S3B′) and astrocytes (white arrowhead, Figure S3B′), hippocampal cells (Figure S3B″), as well as cells in proximity to the ventricular region (Figure S3B″).

DISCUSSION

This study demonstrates the remarkable ability of a single i.v. injection of an AAV-hamartin vector to substantially extend the lifespan of homozygous *Tsc1*-floxed mice that have lost hamartin in a subset of neural cells throughout the brain starting from birth due to an i.c.v. injection of AAV1-Cre. This stochastic loss of hamartin in the mouse brain leads to enlarged neurons, cortical heterotopias, SEN-like overgrowths of the subependymal layer of the ventricles, enlarged ventricles, and hydrocephalus, with hydrocephalus thought to contribute to early death.[11] Using two different serotypes of AAV, rh8 and 9, both of which can enter the brain following i.v. administration,[12,13] an i.v. injection of AAV-hamartin at P21 extended the lifespan of most of these mice an average of 156 and over 429 days, respectively, with a normal lifespan of these mice being about 650 days. Extended lifespan was accompanied by resolution of subventricular overgrowths and reduction in size of ventricles, return of most neuronal cells in the brain to a normal size, and apparent normalization of levels of S6 phosphorylation in the brain. One of the advantages of this gene therapy approach is that the cDNA for

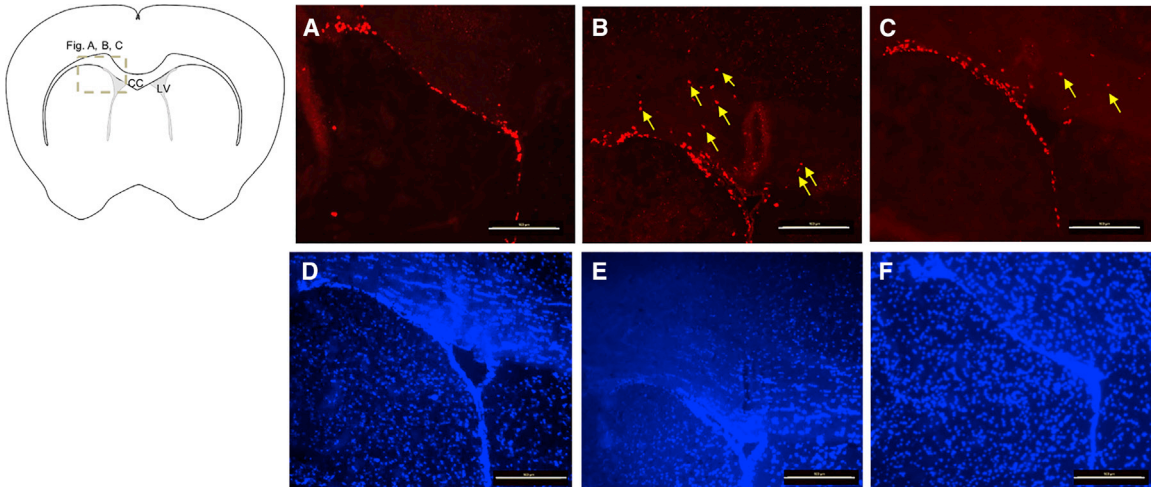

Figure 4. Ki67 Immunostaining of *Tsc1*-Floxed Brains

(A–C) Tsc1-floxed mice injected with AAV1-Cre vectors only show more proliferating cells adjacent to the lateral ventricular area (B) as compared with the naive group (A) and the Tsc1-floxed mice rescued by AAV9-hamartin vectors (C). Yellow arrows indicate the proliferating Ki67+ve cells some distance away from the ventricular layer. The corresponding brain sections were counterstained with DAPI (D–F). Original magnification, ×20. Scale bar, 100 μm. CC, corpus callosum; LV, lateral ventricle.

full-length hamartin is 3.5 kb, and thus fits easily into the 4.6-kb capacity of an AAV vector as a self-complementary vector that provides robust transgene expression.[16] In addition, a single injection, sometime after the disease course has been set, suffices for a remarkable extension of lifespan. AAV9 vectors in clinical trials for neurological diseases in humans are showing long-term benefits with low-to-no adverse effects.[17] Because TSC1/hamartin is thought to function largely, if not exclusively, in a complex with TSC2/tuberin and TBC1D7,[18] and levels of tuberin are normal in these mice, overexpression of hamartin was predicted to have no adverse effects, and none were noted.

Current treatment for symptoms of TSC is based on rapamycin analogs that inhibit mTORC1 activity. Although these analogs are effective for some symptoms, they require continuous treatment, have reduced access to the brain from the periphery,[19] compromise immune function,[20–22] and may interfere with neuronal development.[23,24] AAV vectors have recently become a clinical product for treatment of eye disease (Luxturna; Spark Therapeutics) and spinal muscular atrophy (Zolgensma; Novartis), and they hold great promise for single application benefit in patients with hereditary diseases caused by loss of protein function. In the case of gene replacement of hamartin, there appears to be no toxic effect on cells expressing normal levels of hamartin, probably because hamartin needs to complex with tuberin to be active and is therefore titrated by the normal levels of tuberin present in *Tsc1*-floxed cells.

Clinical trials with the AAV-hamartin vector may be facilitated by the fact that reduction in size of SENs should be relatively rapid and can be monitored by MRI.[25,26] Subependymal nodule can expand into SEGAs and occur in 10%–15% of TSC children, usually appearing after birth.[25,26] These can enlarge over the first decade of life, causing obstruction of cerebrospinal fluid flow, leading to life-threatening hydrocephalus, as well as endocrinopathy and visual impairment. Under optimal care, TSC infants and children are monitored for subependymal lesions by MRI every 6–12 months. The two current standard of care procedures are neurosurgical removal of the SEGA through craniotomy, which is associated with significant morbidity,[26] or treatment with the rapamycin analog, everolimus, which has concerns, especially in children for whom arguably it may interfere with normal brain development. In development, the hamartin and tuberin complex serves to regulate the mTORC1 pathway, which is critical to neuronal growth, axon guidance, synapse formation, and myelination.[6,7,24] Increased mTOR activity has also been associated with ectopic neuronal differentiation, enlarged neurons with increased dendritic complexity, defects in neuronal migration and cortical malfomations.[7,27] On the other hand, inhibition of mTOR by rapamycin appears to contribute to the observed memory dysfunction in the prenatal and post-natal drug treatment in Tsc mouse models[23] and the behavioral abnormalities in wild-type mice treated prenatally with rapamycin.[6] Further, rapamycin treatment for TSC lesions must be continuous or lesions will resume growth. Alternately, because AAV9 and AAVrh8 vectors cross the BBB, the AAV-hamartin vector could be administered i.v., as has been done to rescue motor neurons in spinal muscular atrophy patients.[28] This could have the added advantage of providing extra levels of hamartin in heterozygous TSC1 cells, which might, in turn, reduce the effects of a subsequent somatic mutation in the normal TSC1 gene, leading to growth of lesions in the brain and in other parts of the body. It is hoped that gene replacement therapy may reduce use of current problematic standard of care procedures in young children with TSC1 and provide long-lasting benefit. This AAV-mediated gene therapy could also be combined with rapamycin therapy for lesions arising later in life.

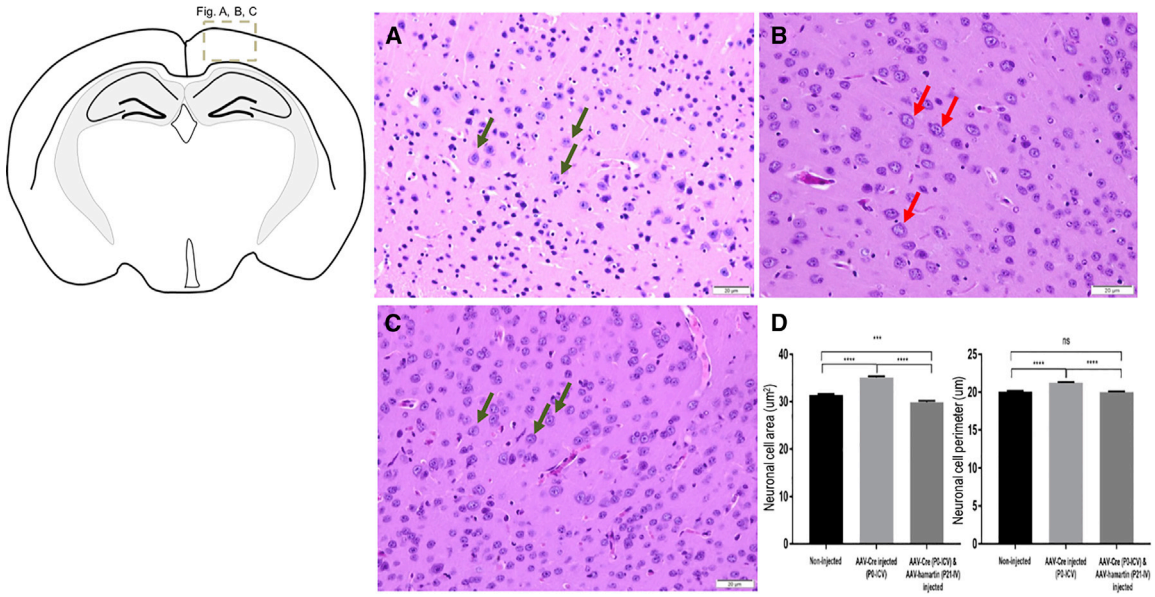

Figure 5. H&E Staining of Brain Sections and Measurement of Diameter of the Neurons

(A and C) Normal size of neurons (green arrows) was observed in the cerebral cortical region above the lateral ventricles on P37 in non-injected *Tsc1*-floxed mice (A) and in AAV1-Cre (P0) and AAV9-hamartin (P21) vector-injected mice (C). (B) Large neurons (red arrows) were observed in the brains injected with AAV-Cre only. Original magnification, ×40. Scale bars, 20 μm. (D) The perimeter (μm) and area size (μm^2) of randomly selected neuronal cell bodies were measured in 540 neurons in the cortex from several fields with three animals per group, and the observer was blinded to group status. Data are shown as mean ± SEM (***$p < 0.001$; ****$p < 0.0001$).

Conclusions

In this preclinical study of gene replacement therapy in a mouse model of TSC1, AAV vectors that cross the BBB, such as serotypes rh8 and 9, encoding hamartin were able to increase survival time by at least 3-to 13-fold. Increase in survival was accompanied by normalization of sizes of ventricles and neural cell bodies in the brain.

MATERIALS AND METHODS

AAV Vector Design and Packaging

AAV vector plasmid, AAV-CBA-Cre-BGHpA, was derived from the plasmid AAV-CBA-EGFP-W[14] by replacing EGFP and Woodchuck hepatitis virus (WHP) posttranscriptional regulatory element (WPRE) element with cDNA encoding Cre recombinase. The AAV-CBA-GFP-W vector was used as a control. The CBA promoter is composed of the CMV immediate or early gene enhancer fused to the β-actin promoter.[8] The dsCMV-hamartin-c-Myc plasmid was derived from the double-stranded AAV (dsAAV)-CBA-BGHpA. This plasmid carries two AAV2 ITR elements, one wild-type and one in which the terminal resolution site was deleted, as described previously,[14] generating a vector that is packaged as a double-stranded molecule. This AAV-CMV-hamartin-c-Myc construct[9] was generated by replacing the CBA promoter in the parent plasmid with PCR-amplified CMV promoter using a lentivirus vector construct[29] as a template and the following primers: CMV-1: 5′-AAAGGTACCGATTAATAGTAATCAATTACGGGGT-3′ and CMV-2: 5′-AGCGCTAGCGGATCTGACGGTTCACT-3′ inserted in between KpnI and NheI sites. Human hamartin cDNA was PCR amplified using the original human hamartin plasmid TSC1-FLAGpcDNA[30] as a template and the following primers: hamartin-1: 5′-AAAGCTAGCGCCACCATGGCCCAACAAGCAAATGTCGGGGA-3′ and hamartin-2: 5′-AAAAGCGGCCGCTTAGCTGTGTTCATGATGAGTCTCATTG-3′ and inserted in between NotI and SacI sites. The c-Myc epitope was added in-frame at the C terminus by using the following primer: 5′-AAGCGGCCGCTCACAGGTCCTCCTCGCTGATCAGCTTCTGCTCGCTGTGTTCATGATGAGTCTCATTG-3′.

AAVrh8, AAV9, and AAV1 serotype vectors were produced by transient co-transfection of 293T cells by calcium phosphate precipitation of vector plasmids (AAV-CMV-hamartin) or Cre,[14] adenoviral helper plasmid pFΔ6, and a plasmid encoding AAVrh8 (pAR-rh8), AAV9 (pXR9), or AAV1 (pXR1) capsid genes, as previously described.[14] All AAV vectors carried the bovine growth hormone polyadenylation signal. The identity of all PCR-amplified sequences was confirmed by sequencing. In brief, AAV vectors were purified by iodixanol gradient centrifugation followed by column chromatography using HiTrapQ anion exchange columns (GE Healthcare, Piscataway, NJ, USA). The virus-containing fractions were concentrated using Centricon 100-kDa molecular weight cut-off (MWCO) centrifugal devices (EMD Millipore, Billerica, MA, USA), and the titer (g.c./mL) was determined by real-time PCR amplification with primers and a probe specific for the bovine growth hormone polyadenylation (BGH polyA) sequences.

Animals and Injections

Experimental research protocols were approved by the Institutional Animal Care and Use Committee (IACUC) for the Massachusetts General

Hospital (MGH) following the guidelines of the NIH's *Guide for the Care and Use of Laboratory Animals*. Experiments were performed on $Tsc1^{c/c}$ mice (*Tsc1*-floxed), which also carried the Cre-inducible ROSA26 *lacZ* marker allele, as described previously.[10,31] In response to Cre recombinase, the $Tsc1^{c/c}$ alleles are converted to null alleles.

These *Tsc1*-floxed mice have a normal lifespan. For i.c.v. vector injections, shortly after birth (P0–P3) neonates were cryo-anesthetized and injected with 2 μL viral vector AAV1-CBA-Cre into each cerebral lateral ventricle with a glass micropipette (70–100 mm in diameter at the tip) using a Narishige IM300 microinjector at a rate of 2.4 psi/s (Narshige International, East Meadow, NY, USA). Mice were then placed on a warming pad and returned to their mothers after regaining normal color and full activity typical of newborn mice.

For retro-orbital injections, at 3 weeks of age (P21) mice were anesthetized with isoflurane inhalation (3.5% isoflurane in an induction chamber and then maintained anesthesia with 2%–3% isoflurane and 1–2 L/min O_2 for the duration of the experiment). AAV vectors were injected retro-orbitally into the vasculature right behind one of the eyeballs in a volume of 60 μL (10 μL AAVrh8 or AAV9-CMV-hamartin or AAVrh8-GFP and 50 μL 0.9% saline) using a 0.3-mL insulin syringe over a 30-s to 2-min period.[32]

We also evaluated the efficiency of AAV1-mediated delivery of Cre-recombinase to brain cells. P1 pups of the floxed reporter mouse [$Gt(ROSA)26Sor^{tm9(CAG\text{-}tdTomato)Hze}$] were injected with 2 μL of AAV1-CBA-Cre (1.8×10^{11} g.c.) via i.c.v. injection into each ventricle. We further evaluated the efficiency of AAV9-mediated delivery of GFP to brain cells via i.v. injection. P21 pup of the C57/BL6 strain was injected with 60 μL AAV9-CBA-GFP (1.8×10^{11} g.c.) via retro-orbital injection.

Body Weight Measurement and Functional Assessment of Motor Activity

Mice at P23 consisting of both genders were subjected to body weight measurement and motor function assessment (n = 5 for naive group [male = 2; female = 3], n = 6 for AAV1-CBA-Cre injection at P1 [male = 2; female = 4], n = 7 for AAV1-CBA-Cre injection at P1 and AAV9-hamartin injection at P21 [male = 3; female = 4]). Sixteen measurements of the body weight of the animals were recorded from P23 to P43. To assess motor co-ordination, animals were placed on an automated rotarod apparatus (Harvard Apparatus, Holliston, MA, USA) using accelerated (4–64 rpm over 120 s) velocities. Each animal was assessed three times with 5-min rest intervals in each session. In each case, the experiment ended when the mouse fell off the treadmill or when the total time elapsed. Seven measurements of the motor function assessment of the animals were recorded from P23 to P43. All functional assessment tests were performed blinded with respect to the mouse genotype.

Histology and Immunohistochemistry (IHC) for Paraffin Sections

For standard histology, mice were first euthanized with CO_2 followed by immediate removal of brain and 2–4 days of fixation in Bouin's solution (VWR International, Radnor, PA, USA). Following paraffin embedding, 5-μm sections were stained with H&E and examined for full-body pathology by R.T.B., including chest, trachea, lungs, heart, kidneys, spleen, pancreas, spinal cord, and reproductive organ, using three mice per group. Five-micrometer coronal sections from the brain were stained with H&E or were used for IHC. Sections were deparaffinized in xylenes followed by re-hydration in decreasing ethanol concentrations. Endogenous peroxidase was blocked with 3% hydrogen peroxide; then tissues were washed in PBS. Heat-induced antigen retrieval was performed using sodium citrate (10 mM, pH 6.0) in a 95°C water bath for 10 min. Tissues were blocked in 5% normal goat serum, then incubated with primary antibody pS6 235/236 (#2211; Cell Signaling, Danvers, MA, USA) diluted 1:450, at 4°C overnight. On the next day, the brain sections were washed in Tris-buffered saline and Tween 20 (TBST) three times at 3-min intervals. Tissues were then incubated with ready-to-use secondary antibody, SignalStain Boost IHC Detection Reagent (#8114; Cell Signaling), at room temperature (RT) for 30 min, and washed in TBST three times at 3-min intervals. The sections were then incubated with DAKO horseradish peroxidase (HRP)-compatible DAB (Vector Laboratories, Burlingame, CA, USA) for 3 min, washed with water, and then counterstained with hematoxylin, dehydrated, mounted, and preserved with coverslips. Semi-quantitative analysis of pS6 staining intensity in cerebral cortex was evaluated by a blinded observer on a scale of 0–3 (0 for no staining, 1 for light or weak staining, 2 for moderate staining, and 3 for strong and intense staining). Brain sections were stained for the c-Myc tag to detect transgene delivery but the current lots of c-Myc antibody (#1667149, Roche Diagnostics) did not detect a signal.

Neuronal Cell Measurements

H&E-stained brain sections were imaged on a Olympus microscope at a magnification of ×40, and images were captured from the cerebral cortex above the lateral ventricles, as suggested by the pathologist (A.S.-R.), because these regions appeared to have the most notable differences in size of the neurons as compared among these sets of mice. The neurons were characterized by prominent nucleolus within the pale staining nucleus and the cytoplasm.[15] Images were examined using ImageJ. The perimeter (μm) and area size (μm^2) were measured for 540 randomly selected neurons from several fields of the cerebral cortical region with three animals per group by an observer blinded to status. Data are shown as mean ± SEM (***$p < 0.001$; ***$p < 0.0001$).

Histology and IHC for Frozen Sections

Adult mice were euthanized using ketamine/xylazine (100:10) followed by transcardiac perfusion with 1× PBS and 4% paraformaldehyde in PBS overnight at 4°C, cryoprotected with 25% sucrose in PBS, and embedded in tissue-embedding medium. Brain sections were prepared in 10-μm coronal sections and were blocked in 10% BSA in PBST (0.1× PBS+0.3% Triton X-100) for 1 h at RT and subsequently incubated with rabbit anti-Ki67 (#ab15580, 1:1,000; Abcam) overnight at RT. Following three washes in 0.1× PBS, the sections

were incubated with secondary antibodies for 1 h at RT. The sections were then washed three times with 0.1× PBS and mounted with DAPI mounting medium (Vectashield, #H-1200).

IHC for Free-Floating Brain Sections

To evaluate the efficiency of AAV1-mediated delivery of Cre-recombinase to brain cells, we injected P1 pups of the floxed reporter mouse [Gt(ROSA)26Sor$^{tm9(CAG-tdTomato)Hze}$] (JAX#008848; Jackson Labs)[33] with AAV1-CBA-Cre i.c.v. The pups were euthanized at P21 with transcardiac perfusion with 1× PBS followed by 4% paraformaldehyde in PBS overnight at 4°C, cryoprotected with 25% sucrose in PBS, and embedded in optimal cutting temperature (OCT) tissue-embedding medium. Free-floating brain sections were prepared as 40-μm coronal sections, and endogenous fluorescent signal was detected using a tetramethylrhodamine isothiocyanate (TRITC) filter with fluorescent microscopy.

We further evaluated the efficiency of AA9-mediated delivery of GFP to brain cells via i.v. injection. P21 pups of the C57/BL6 strain were injected with AAV9-CBA-GFP via retro-orbital injection. Two weeks later, the animal was euthanized at P35 with transcardiac perfusion with PBS followed by 4% paraformaldehyde in PBS for 48 h at 4°C, cryoprotected with 25% sucrose in PBS, and embedded in OCT tissue-embedding medium. Free-floating brain sections were prepared in 40-μm coronal sections and permeabilized with 0.5% Triton-X in PBS. The sections were blocked in 5% normal goat serum in PBS for 1 h at RT and subsequently incubated with GFP primary antibody (#G10362, 1:400 dilution; Invitrogen) for 5 days at 4°C on shaker. Following three washes in PBS, the sections were incubated with secondary antibody (goat anti-rabbit IgG Alexa 488, #A-11034, 1:1,000 dilution) for 1 h at RT.

Statistical Analysis

All analyses of survival curves (chi-square test) were performed using GraphPad Prism software (GraphPad Software, La Jolla, CA, USA). The p values depicted are statistically significant. Diameter and perimeter of the neurons were quantitatively analyzed using ImageJ software and plotted in GraphPad Prism. One-way ANOVA followed by Tukey's post hoc test was used to evaluate statistical significance of intensity levels of pS6 staining.

SUPPLEMENTAL INFORMATION

Supplemental Information can be found online at https://doi.org/10.1016/j.omtm.2019.08.003.

AUTHOR CONTRIBUTIONS

X.O.B., S.P., M.S.-E., D.J.K., and C.A.M. conceived and designed the experiments; S.P., X.Z., B.A.T., and P.S.C. performed the experiments; S.P., R.T.B., P.S.C., and A.S.-R. analyzed the data; S.P. and X.O.B. wrote and edited the paper.

CONFLICTS OF INTEREST

The authors declare no competing interests.

ACKNOWLEDGMENTS

We thank Suzanne McDavitt for her skilled editorial assistance; Osama Mardini for his technical help with the injections; Michelle Forrestall Lee, Medical Photographer in Pathology Media Lab, MGH, for the imaging training; Kevin Conway, Vector Core, MGH, Charlestown, MA, USA, for AAV vectors packaging; Dakai Mu, MGH, Charlestown, MA, USA, for virus vector packaging, and Dr. Michael Whalen for the use of rotarod. This work was supported by NIH/NINDS grant NS024279, DOD Army Grant W81XWH-13-1-0076, NIH NINDS grant P30 NS045776, and DOD Army Grant W81XWH-16-1-0134.

REFERENCES

1. Henske, E.P., Jóźwiak, S., Kingswood, J.C., Sampson, J.R., and Thiele, E.A. (2016). Tuberous sclerosis complex. Nat. Rev. Dis. Primers *2*, 16035.
2. Huang, J., and Manning, B.D. (2009). A complex interplay between Akt, TSC2 and the two mTOR complexes. Biochem. Soc. Trans. *37*, 217–222.
3. Crino, P.B. (2013). Evolving neurobiology of tuberous sclerosis complex. Acta Neuropathol. *125*, 317–332.
4. Kwiatkowski, D.J., Whittemore, V.H., and Thiele, E.A. (2010). Tuberous Sclerosis Complex: Genes, Clinical Features, and Therapeutics (Wiley-Blackwell).
5. Kandt, R.S. (2003). Tuberous sclerosis complex and neurofibromatosis type 1: the two most common neurocutaneous diseases. Neurol. Clin. *21*, 983–1004.
6. Tsai, P.T., Greene-Colozzi, E., Goto, J., Anderl, S., Kwiatkowski, D.J., and Sahin, M. (2013). Prenatal rapamycin results in early and late behavioral abnormalities in wild-type C57BL/6 mice. Behav. Genet. *43*, 51–59.
7. Sokolov, A.M., Seluzicki, C.M., Morton, M.C., and Feliciano, D.M. (2018). Dendrite growth and the effect of ectopic Rheb expression on cortical neurons. Neurosci. Lett. *671*, 140–147.
8. Gray, S.J., Foti, S.B., Schwartz, J.W., Bachaboina, L., Taylor-Blake, B., Coleman, J., Ehlers, M.D., Zylka, M.J., McCown, T.J., and Samulski, R.J. (2011). Optimizing promoters for recombinant adeno-associated virus-mediated gene expression in the peripheral and central nervous system using self-complementary vectors. Hum. Gene Ther. *22*, 1143–1153.
9. Prabhakar, S., Zhang, X., Goto, J., Han, S., Lai, C., Bronson, R., Sena-Esteves, M., Ramesh, V., Stemmer-Rachamimov, A., Kwiatkowski, D.J., and Breakefield, X.O. (2015). Survival benefit and phenotypic improvement by hamartin gene therapy in a tuberous sclerosis mouse brain model. Neurobiol. Dis. *82*, 22–31.
10. Meikle, L., Talos, D.M., Onda, H., Pollizzi, K., Rotenberg, A., Sahin, M., Jensen, F.E., and Kwiatkowski, D.J. (2007). A mouse model of tuberous sclerosis: neuronal loss of Tsc1 causes dysplastic and ectopic neurons, reduced myelination, seizure activity, and limited survival. J. Neurosci. *27*, 5546–5558.
11. Prabhakar, S., Goto, J., Zhang, X., Sena-Esteves, M., Bronson, R., Brockmann, J., Gianni, D., Wojtkiewicz, G.R., Chen, J.W., Stemmer-Rachamimov, A., et al. (2013). Stochastic model of Tsc1 lesions in mouse brain. PLoS ONE *8*, e64224.
12. Foust, K.D., Nurre, E., Montgomery, C.L., Hernandez, A., Chan, C.M., and Kaspar, B.K. (2009). Intravascular AAV9 preferentially targets neonatal neurons and adult astrocytes. Nat. Biotechnol. *27*, 59–65.
13. Yang, B., Li, S., Wang, H., Guo, Y., Gessler, D.J., Cao, C., Su, Q., Kramer, J., Zhong, L., Ahmed, S.S., et al. (2014). Global CNS transduction of adult mice by intravenously delivered rAAVrh.8 and rAAVrh.10 and nonhuman primates by rAAVrh.10. Mol. Ther. *22*, 1299–1309.
14. Broekman, M.L., Comer, L.A., Hyman, B.T., and Sena-Esteves, M. (2006). Adeno-associated virus vectors serotyped with AAV8 capsid are more efficient than AAV-1 or -2 serotypes for widespread gene delivery to the neonatal mouse brain. Neuroscience *138*, 501–510.
15. Garman, R.H. (2011). Histology of the central nervous system. Toxicol. Pathol. *39*, 22–35.

16. McCarty, D.M., Monahan, P.E., and Samulski, R.J. (2001). Self-complementary recombinant adeno-associated virus (scAAV) vectors promote efficient transduction independently of DNA synthesis. Gene Ther. *8*, 1248–1254.

17. Dunbar, C.E., High, K.A., Joung, J.K., Kohn, D.B., Ozawa, K., and Sadelain, M. (2018). Gene therapy comes of age. Science *359*, eaan4672.

18. Dibble, C.C., Elis, W., Menon, S., Qin, W., Klekota, J., Asara, J.M., Finan, P.M., Kwiatkowski, D.J., Murphy, L.O., and Manning, B.D. (2012). TBC1D7 is a third subunit of the TSC1-TSC2 complex upstream of mTORC1. Mol. Cell *47*, 535–546.

19. Chi, O.Z., Kiss, G.K., Mellender, S.J., Liu, X., and Weiss, H.R. (2017). Rapamycin decreased blood-brain barrier permeability in control but not in diabetic rats in early cerebral ischemia. Neurosci. Lett. *654*, 17–22.

20. Almeida, F., Amorim, S., Sarmento, A., and Santos, L. (2018). Life-threatening everolimus-associated pneumonitis: a case report and a review of the literature. Transplant. Proc. *50*, 933–938.

21. Barbari, A., Maawad, M., Kfoury Kassouf, H., and Kamel, G. (2015). Mammalian target of rapamycin inhibitors and nephrotoxicity: fact or fiction. Exp. Clin. Transplant. *13*, 377–386.

22. Stucker, F., and Ackermann, D. (2011). [Immunosuppressive drugs—how they work, their side effects and interactions]. Ther. Umsch. *68*, 679–686.

23. Way, S.W., Rozas, N.S., Wu, H.C., McKenna, J., 3rd, Reith, R.M., Hashmi, S.S., Dash, P.K., and Gambello, M.J. (2012). The differential effects of prenatal and/or postnatal rapamycin on neurodevelopmental defects and cognition in a neuroglial mouse model of tuberous sclerosis complex. Hum. Mol. Genet. *21*, 3226–3236.

24. Ryskalin, L., Lazzeri, G., Flaibani, M., Biagioni, F., Gambardella, S., Frati, A., and Fornai, F. (2017). mTOR-dependent cell proliferation in the brain. BioMed Res. Int. *2017*, 7082696.

25. DiMario, F.J., Jr. (2004). Brain abnormalities in tuberous sclerosis complex. J. Child Neurol. *19*, 650–657.

26. Kotulska, K., Borkowska, J., Roszkowski, M., Mandera, M., Daszkiewicz, P., Drabik, K., Jurkiewicz, E., Larysz-Brysz, M., Nowak, K., Grajkowska, W., et al. (2014). Surgical treatment of subependymal giant cell astrocytoma in tuberous sclerosis complex patients. Pediatr. Neurol. *50*, 307–312.

27. Lafourcade, C.A., Lin, T.V., Feliciano, D.M., Zhang, L., Hsieh, L.S., and Bordey, A. (2013). Rheb activation in subventricular zone progenitors leads to heterotopia, ectopic neuronal differentiation, and rapamycin-sensitive olfactory micronodules and dendrite hypertrophy of newborn neurons. J. Neurosci *33*, 2419–2431.

28. Parente, V., and Corti, S. (2018). Advances in spinal muscular atrophy therapeutics. Ther. Adv. Neurol. Disorder. *11*, 1756285618754501.

29. Sena-Esteves, M., Tebbets, J.C., Steffens, S., Crombleholme, T., and Flake, A.W. (2004). Optimized large-scale production of high titer lentivirus vector pseudotypes. J. Virol. Methods *122*, 131–139.

30. Franz, D.N., Leonard, J., Tudor, C., Chuck, G., Care, M., Sethuraman, G., Dinopoulos, A., Thomas, G., and Crone, K.R. (2006). Rapamycin causes regression of astrocytomas in tuberous sclerosis complex. Ann. Neurol. *59*, 490–498.

31. Mao, X., Fujiwara, Y., and Orkin, S.H. (1999). Improved reporter strain for monitoring Cre recombinase-mediated DNA excisions in mice. Proc. Natl. Acad. Sci. USA *96*, 5037–5042.

32. Yardeni, T., Eckhaus, M., Morris, H.D., Huizing, M., and Hoogstraten-Miller, S. (2011). Retro-orbital injections in mice. Lab Anim. (NY) *40*, 155–160.

33. Madisen, L., Zwingman, T.A., Sunkin, S.M., Oh, S.W., Zariwala, H.A., Gu, H., Ng, L.L., Palmiter, R.D., Hawrylycz, M.J., Jones, A.R., et al. (2010). A robust and high-throughput Cre reporting and characterization system for the whole mouse brain. Nat. Neurosci *13*, 133–140.

OMTM, Volume *15*

Supplemental Information

Long-Term Therapeutic Efficacy of Intravenous AAV-Mediated Hamartin Replacement in Mouse Model of Tuberous Sclerosis Type 1

Shilpa Prabhakar, Pike See Cheah, Xuan Zhang, Max Zinter, Maria Gianatasio, Eloise Hudry, Roderick T. Bronson, David J. Kwiatkowski, Anat Stemmer-Rachamimov, Casey A. Maguire, Miguel Sena-Esteves, Bakhos A. Tannous, and Xandra O. Breakefield

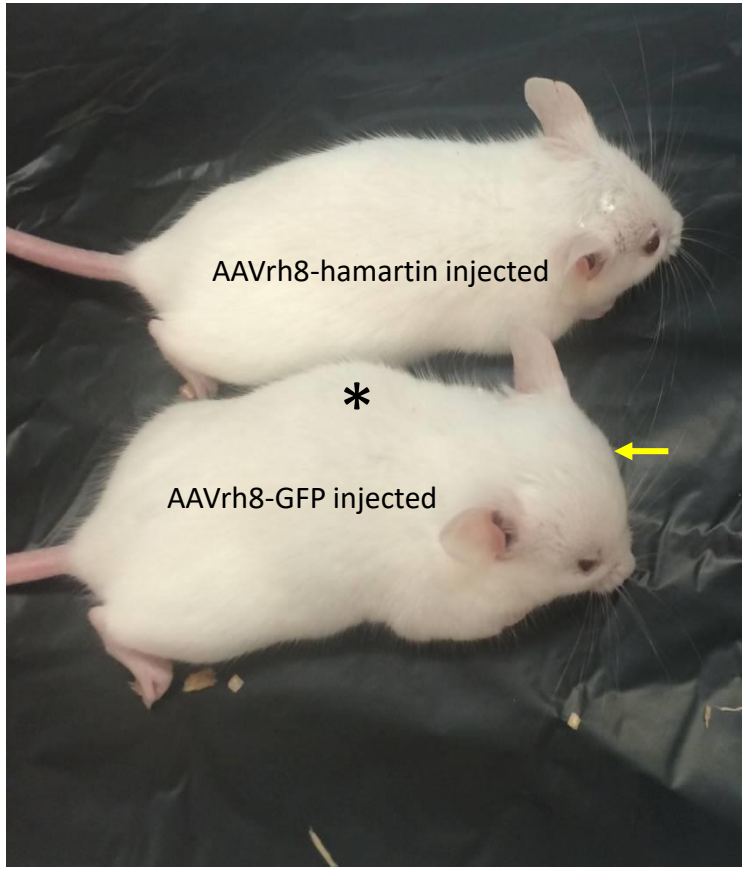
AAVrh8-hamartin injected
*
AAVrh8-GFP injected

Supplementary Fig. S1. Appearance of mice. Both *Tsc1*-floxed pups were injected at P0 ICV with AAV-Cre vector and at day 21, one of the mice were injected IV via retro-orbital vasculature with AAVrh8-hamartin or AAVrh8-GFP. At P46, GFP-injected mouse showed a swollen head (yellow arrowhead) and hunched posture (*), while the hamartin-injected mouse looked normal. Representative mice are shown.

Fig. A, B, C

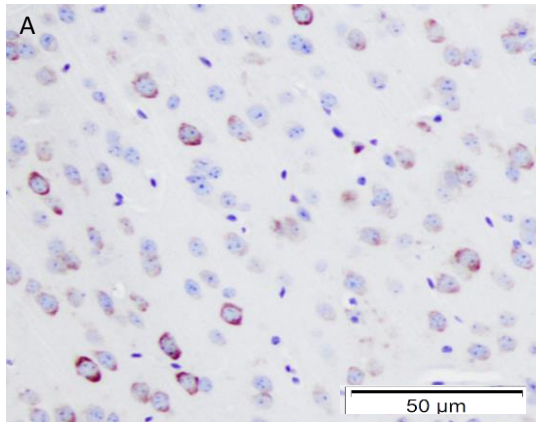
A
50 µm

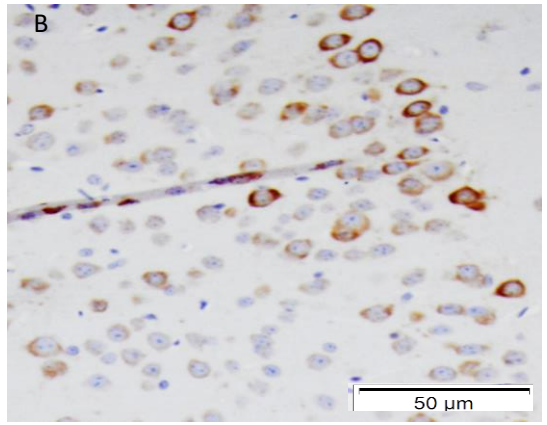
B
50 µm

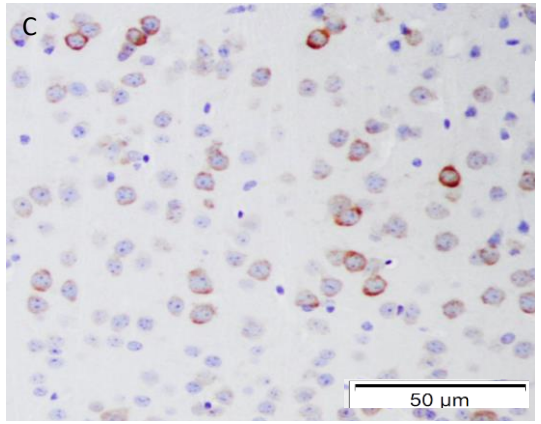
C
50 µm

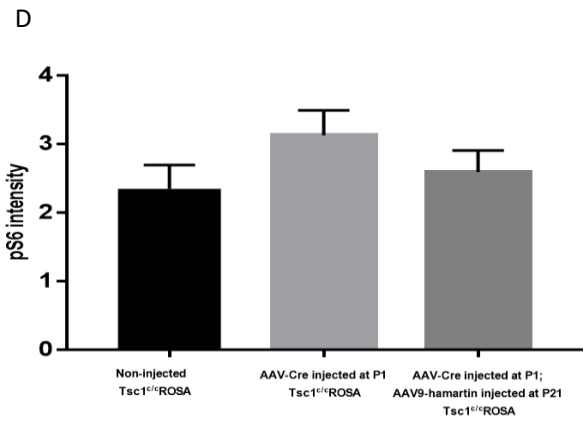
D
pS6 intensity
0
1
2
3
4
Non-injected
Tsc1c/cROSA
AAV-Cre injected at P1
Tsc1c/cROSA
AAV-Cre injected at P1;
AAV9-hamartin injected at P21
Tsc1c/cROSA

Supplementary Fig. S2. pS6 immunostaining of *Tsc1*-floxed brain sections. Staining of brains with pS6 shows that cell bodies of neurons in the cortical region right above the above the lateral ventricles on day 37: normal (brown) staining in non-injected *Tsc1*-floxed mice (A); apparently elevated staining in the AAV-Cre-injected *Tsc1*-floxed mice (B); and reduced levels staining appearing in the AAV-Cre-injected *Tsc1*-floxed mice rescued by single injection of AAV9-hamartin vector (C). Magnification = 20 X; scale bar = 50 μm. (D) Quantitative analysis of pS6 staining in cerebral cortex of the 3 groups (n=3 each group) using one-way ANOVA followed by Tukey's *post hoc* test revealed non-significant differences in pS6 intensity among groups, p = 0.5423. Error bars represent SEM.

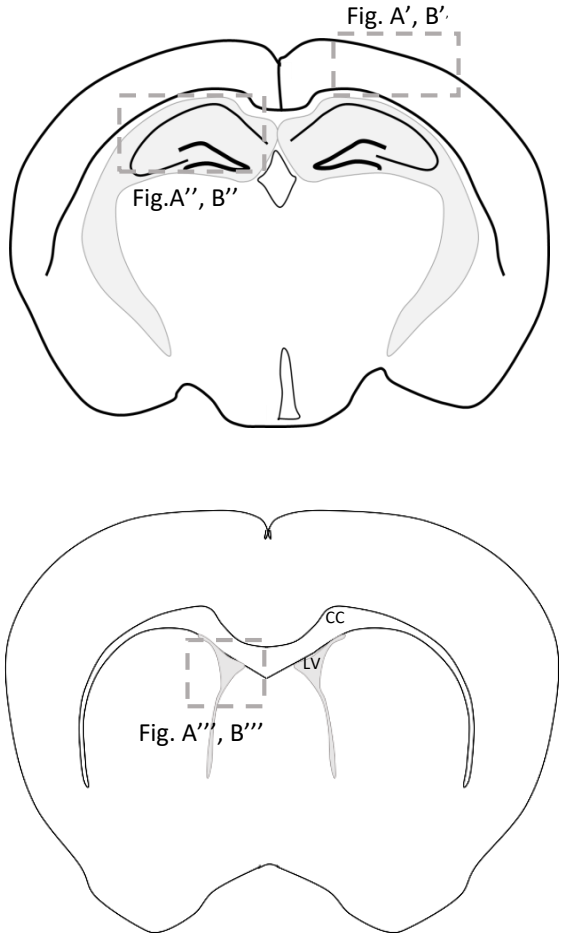
Fig. A', B'
Fig.A'', B''
CC
LV
Fig. A''', B'''

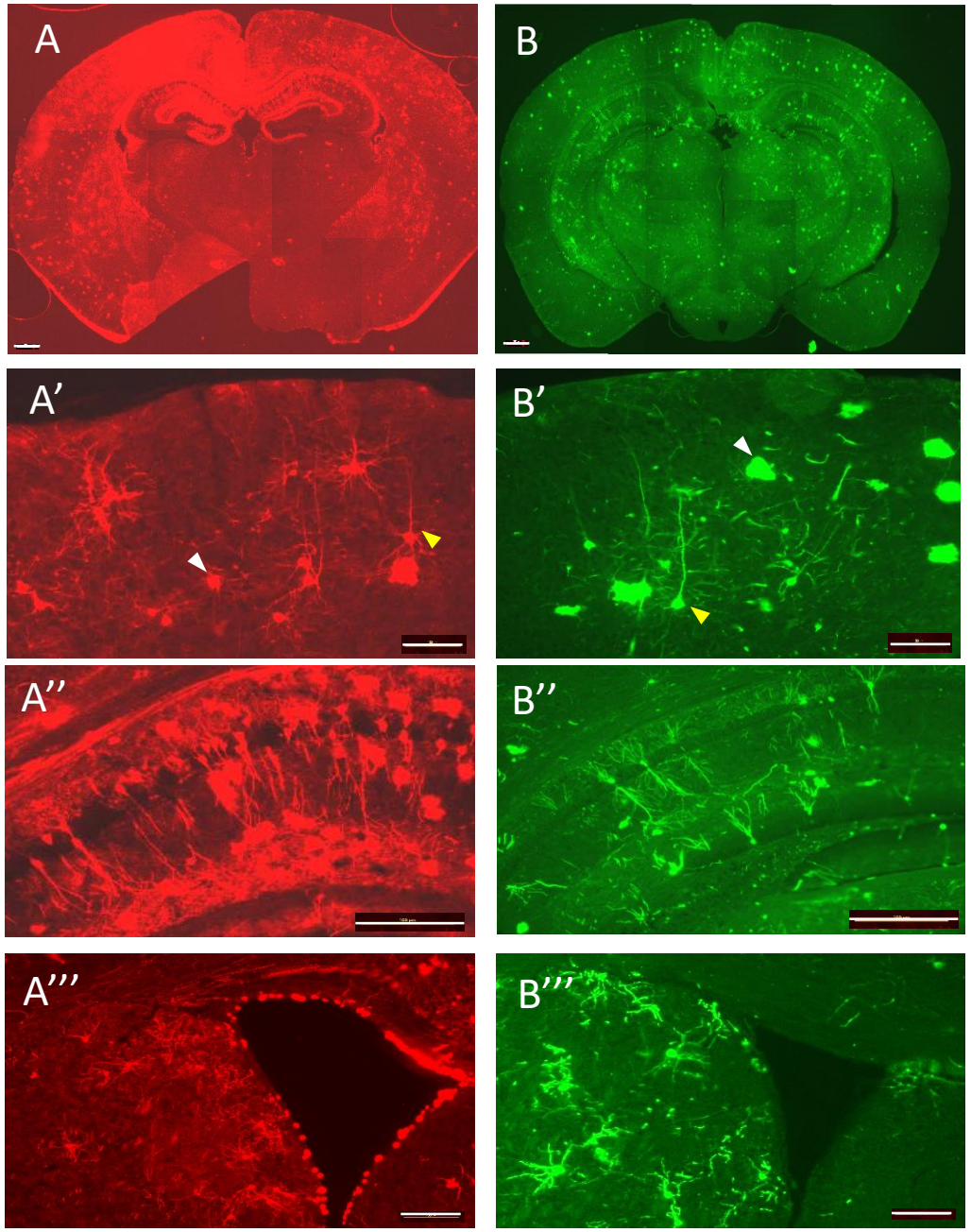
A
B
A'
B'
A''
B''
A'''
B'''

Supplementary Fig. S3. Efficient AAV1 mediated delivery of Cre-recombinase to brain cells via neonatal ICV injection, and of AAV9 delivery of GFP via IV injection into retro-orbital vein. (A) Floxed reporter mice [Gt(ROSA)26Sor$^{tm9(CAG-tdTomato)Hze}$] were injected ICV with AAV1-Cre vector at P1 and brains were cryosectioned at P21. (A) Coronal section of the brain shows expression of tdTomato throughout the brain in what appear to be (A') cortical neuron (yellow arrowhead), (A') astrocyte (white arrowhead), (A'') hippocampal neurons and (A''') cells adjacent to the ventricles. (B) Tsc2$^{c/c}$ mice pups were injected with AAV9-GFP vector at P21 via retro-orbital vasculature and brains were cryosectioned at P35. (B) Coronal section of the brain reveals abundant of GFP-positive cells throughout the brain including what appear to be (B') cortical neuron (yellow arrowhead), (B') astrocyte (white arrowhead), (B'') hippocampal neurons, and (B''') cells in proximity to the lateral ventricle. (A, B: magnification = 4X, scale bar = 200 μm; A', B', A'', B'', A''' & B''': magnification = 20X, scale bar = 100 μm).